Journal of Thermal Analysis and Calorimetry, Vol. 68 (2002) 289–306

THERMAL CHARACTERIZATION AND PHYSICO-CHEMICAL PROPERTIES OF Fe_2O_3–Mn_2O_3/Al_2O_3 SYSTEMS

W. M. Shaheen[1]* *and K. S. Hong*[2]

[1]Physical Chemistry Department, National Research Center, Dokki, Cairo, Egypt
[2]Physics Department, Korean Basic Science Institute, Seoul, 136-701, South Korea

(Received April 5, 2001; in revised form September 19, 2001)

Abstract

The effect of ferric and manganese oxides dopants on thermal and physicochemical properties of Mn-oxide/Al_2O_3 and Fe_2O_3/Al_2O_3 systems has been studied separately. The pure and doped mixed solids were thermally treated at 400–1000°C. Pyrolysis of pure and doped mixed solids was investigated via thermal analysis (TG-DTG) techniques. The thermal products were characterized using XRD-analysis. The results revealed that pure ferric nitrate decomposes into Fe_2O_3 at 350°C and shows thermal stability up to 1000°C. Crystalline Fe_3O_4 and Mn_3O_4 phases were detected for some doped solids precalcined at 1000°C. Crystalline γ-Al_2O_3 phase was detected for all solids preheated up to 800°C. Ferric and manganese oxides enhanced the formation of α-Al_2O_3 phase at 1000°C. Crystalline $MnAl_2O_4$ and $MnFe_2O_4$ phases were formed at 1000°C as a result of solid–solid interaction processes. The catalytic behavior of the thermal products was tested using the decomposition of H_2O_2 reaction.

Keywords: characterization, doping, solid–solid interaction, thermal decomposition

Introduction

The thermal decomposition and the physicochemical properties of the loaded solid are dependent, mainly on many factors such as preparation method [1], the calcination conditions [2], doping with certain foreign cations [3, 4] and also on the extent of loading [5]. Alumina is the most convenient support for the catalysts employed in the oxidation-reduction reactions [6, 7]. This is because of its high surface area, and porous structure [7, 8]. Also, alumina greatly increases the degree of dispersion of the catalytically active constituents, hindering their grain growth and thus increasing the activity and durability of the supported [7–9] catalyst. On the other hand, the combination of transition metal oxides may result in modifications in their thermal behavior, geometric structures and electronic properties that lead to changes in their catalytic functions [10].

---

* Author to whom all correspondence should be addressed.

1418–2874/2002/ $ 5.00

Akadémiai Kiadó, Budapest
Kluwer Academic Publishers, Dordrecht

The present work is devoted to a study of the thermal and the physicochemical properties of manganese nitrate supported on aluminum hydroxide system and ferric nitrate supported on aluminum hydroxide system thermally treated at 400–1000° in the pure state and influenced by doping with different portions of ferric and manganese oxides separately. The techniques employed were thermal analysis (TG-DTG) technique and the X-ray diffraction analysis. The catalytic activities of the calcined pure and doped mixed solids were tested in hydrogen peroxide decomposition reaction at 30, 40 and 50°C.

Experimental

Materials

The starting materials used in this investigation were $Fe(NO_3)_3 \cdot 9H_2O$ and $Mn(NO_3)_2 \cdot 4H_2O$. These chemicals were provided by Fluka Company. $Al(OH)_3$ solid was provided by Prolabo Company. The specific surface area S_{BET} of the employed $Al(OH)_3$ precalcined in air at 500°C for 4 h was determined from the N_2 adsorption isotherm at –196°C and was found to be 235 $m^2 g^{-1}$.

Method of preparation of pure and doped solids

A known mass of finely powdered $Al(OH)_3$ was impregnated with a solution containing definite amount of manganese nitrate tetrahydrate. The obtained pastes were dried at 100°C. A series of the dried pastes were doped with different portions of Fe(III)-nitrate solutions and then dried again at 100°C. The obtained solids were calcined at 400–1000°C for 4 h in air atmosphere.

Table 1 Symbols and the composition of the pure and doped mixtures

Symbols		Composition of pure and doped mixtures fired at 400, 600, 800 and 1000°C (mole/mole)
Mn–Al	I	$0.50Mn(NO_3)_2 \cdot 4H_2O/2.0Al(OH)_3$
Fe–Mn–Al	II	0.05Fe nitrate–0.5Mn nitrate/$2.0Al(OH)_3$
Fe–Mn–Al	III	0.10Fe nitrate–0.5Mn nitrate/$2.0Al(OH)_3$
Fe–Mn–Al	IV	0.20Fe nitrate–0.5Mn nitrate/$2.0Al(OH)_3$
Fe–Mn–Al	V	0.50Fe nitrate–0.5Mn nitrate/$2.0Al(OH)_3$
Fe–Al	VI	$0.50Fe(NO_3)_3 \cdot 9H_2O/2.0Al(OH)_3$
Mn–Fe–Al	VII	0.0.5Mn nitrate–0.5Fe nitrate/$2.0Al(OH)_3$
Mn–Fe–Al	VIII	0.10Mn nitrate–0.5Fe nitrate/$2.0Al(OH)_3$
Mn–Fe–Al	IX	0.20Mn nitrate–0.5Fe nitrate/$2.0Al(OH)_3$
Mn–Fe–Al	X	0.50Mn nitrate–0.5Fe nitrate/$2.0Al(OH)_3$

On the other hand, following the same procedures series of pure mixtures of ferric nitrate supported on aluminum hydroxide and mixtures of it doped with different portions of manganese nitrate were prepared then thermally treated at the same calcination temperatures. The dopant concentration of both nitrates were calculated with respect to Fe_2O_3 and Mn_2O_3 and fixed to be 1.96, 3.85, 7.41 and 16.67 mol% for each other. Table 1 shows the symbols and the composition of the pure and doped mixtures treated at 400, 600, 800 and 1000°C.

Physical measurements

Thermogravimetry (TG) and derivative thermogravimetry (DTG) were carried out on a Shimadzu DT-40 Thermal Analyzer. The sample was placed in platinum crucible (0.1 cm^3). The samples were studied under air atmosphere with flowing rate of 30 mL min^{-1}. The size of samples were selected to be about (7–16 mg). α-Al_2O_3 was used as a reference in this technique. The rate of heating was 10°C min^{-1}.

X-ray diffraction patterns were obtained at room temperature using a Philips X-ray diffractometer (Goniometer PW1050/50), employing CuK_α radiation as the X-ray source. The X-ray tube was operated at 36 kV and 16 mV. Samples were finely ground and packed in a plastic holder. The diffraction angle of 2θ was scanned at a rate of 2°C min^{-1}.

The catalytic decomposition of hydrogen peroxide was used as a model reaction for determining the catalytic activity of pure and doped mixed solids thermally treated at 400, 600, 800 and 1000°C and at reaction temperatures 30, 40 and 50°C. The reaction was followed up through a gasometric measurement of evolved oxygen [10].

Results and discussion

Thermal analysis and XRD-characterization of $Fe(NO_3)_3 \cdot 9H_2O$

Figure 1a shows TG-DTG curves of the pure Fe(III)-nitrate hydrate. It can be seen that, the step starts at about 190°C with a constant mass loss of 78% corresponding to

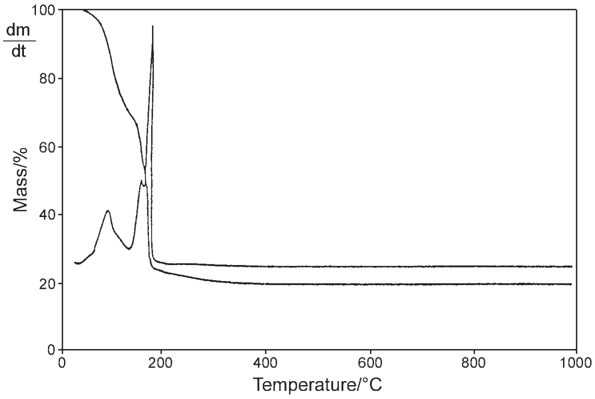

Fig. 1a Thermal analysis (TG-DTG) of pure $Fe(NO_3)_3 \cdot 9H_2O$

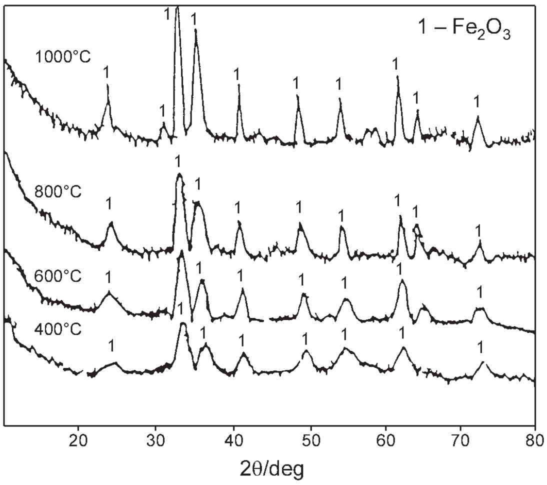

Fig. 1b XR-diffractograms of Fe(III)-nitrate preheated at 400, 600, 800 and 1000°C

the formation of Fe(OOH) [11]. The last step starts at temperature higher than 350°C accompanied by a constant mass loss of 80%, which might characterize the formation of Fe_2O_3 [12] which is thermally stable up to 1000°C.

On the other hand, Fig. 1b represents the X-ray diffractograms of pure ferric nitrate precalcined at 400–1000°C. It shows the formation of α-Fe_2O_3 phase (rhombohedral) [12] at different treatment temperatures. The degree of crystallinity of the formed phase increased with increasing the calcination temperature up to 1000°C.

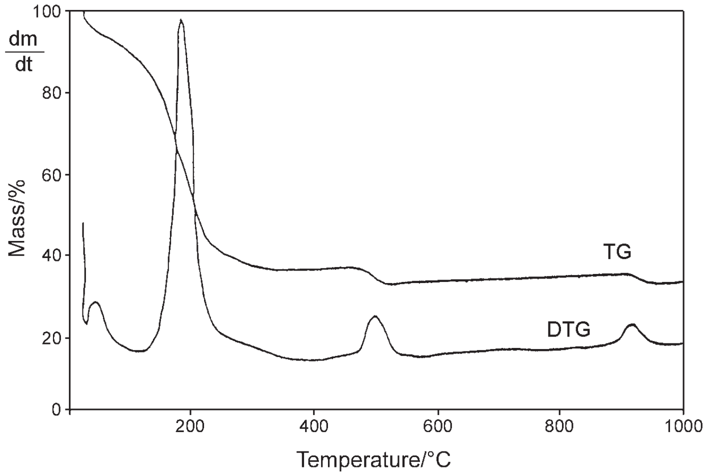

Fig. 1c TG and DTG of pure $Mn(NO_3)_2$·$4H_2O$

Thermal analysis and XRD-characterization of $Mn(NO_3)_2 \cdot 4H_2O$

Figure 1c represents TG and DTG curves of pure manganese nitrate tetrahydrate. The result showed that the pure salt decomposes into MnO_2 [13–14] at about 300°C with a constant mass loss of 65.5%. Then, it converted to Mn_2O_3 at about 500°C with a constant mass loss of 68.5%. The last step starts at about 900°C, and accompanied by a constant mass loss of 70% due to the formation of Mn_3O_4 [10].

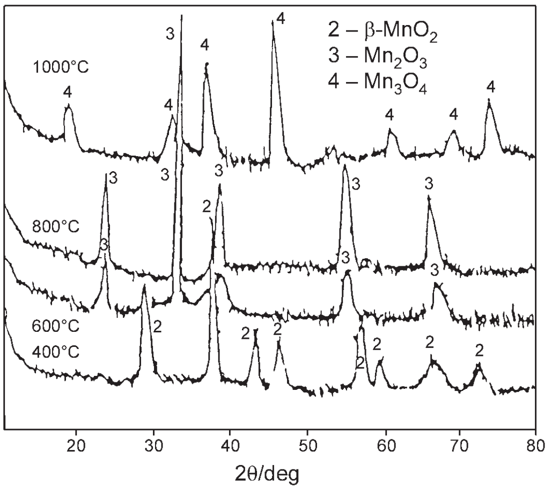

Fig. 1d XR-diffractograms of $Mn(NO_3)_2$ preheated at 400, 600, 800 and 1000°C

On the other hand, the X-ray investigation of pure manganese nitrate; represented in Fig. 1d shows the formation of poorly crystalline β-MnO_2 (tetragonal) phase [13] at 400°C. The thermal treatment of the solid at 600°C yields crystalline Mn_2O_3 (cubic) phase; its degree of crystallinity increased with increasing calcination temperature up to 800°C. The X-ray diffractogram of the thermal treated sample at 1000°C conformed the formation of well crystalline Mn_3O_4 (heximanite) phase [15].

Thermal analysis and XRD-characterization of mixture Mn–Al (I)

Figure 2a showed that TG-DTG curves of the mixture Mn–Al (I) consists of four steps for the thermal decomposition process. The first one starts at 80°C reaching a constant mass loss of 5.5% corresponding to the evolution of water. The second step starts at about 200°C reaching a constant mass loss of 33% at about 425°C corresponding to the formation of manganese dioxide [13] and aluminum oxyhydroxide compound. The third step starts at about 520°C with mass loss of 2.8% which is accompanied by the reduction of manganese dioxide to manganese trioxide and also represents complete decomposition of aluminum oxyhydroxide compound to aluminum oxide. The last step starts at about 880°C reaching a constant total mass loss of 43.5% at about 970°C. This step might represent the conversion of Mn_2O_3 to Mn_3O_4 and the formation of some portion of $MnAl_2O_4$

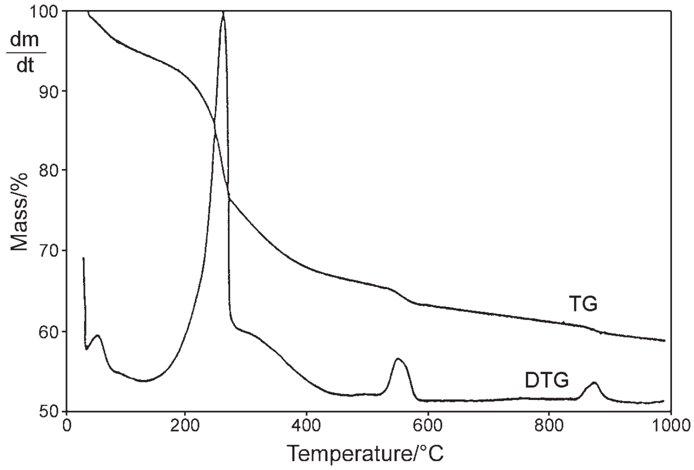

Fig. 2a TG and DTG of mixture Mn–Al (I)

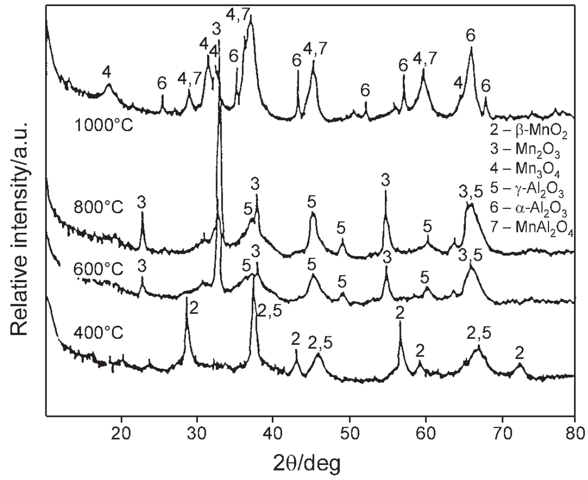

Fig. 2b XR-diffractograms of mixture Mn–Al (I) preheated at 400, 600, 800 and 1000°C

as a result of solid–solid interaction between the corresponding oxides, which will be confirmed later by the XRD investigation of this mixture.

Furthermore, the X-ray investigation of the mixture Mn–Al (I) preheated at 400, 600, 800 and 1000°C are illustrated in Fig. 2b. From this figure, it can be seen that poor crystalline β-MnO_2 and γ-Al_2O_3 phases are detected at 400°C. The pretreatment at 600°C, yielded well crystalline Mn_2O_3 (cubic) phase beside the poorly crystallized γ-Al_2O_3 phase. The degree of crystallinity of both phases increased with increasing the calcination temperature up to 800°C, and is less than that obtained from treatment of pure manganese nitrate at 400–800°C. This might be attributed to the presence of aluminum oxide leading to increase the degree of dispersion of manganese oxides on

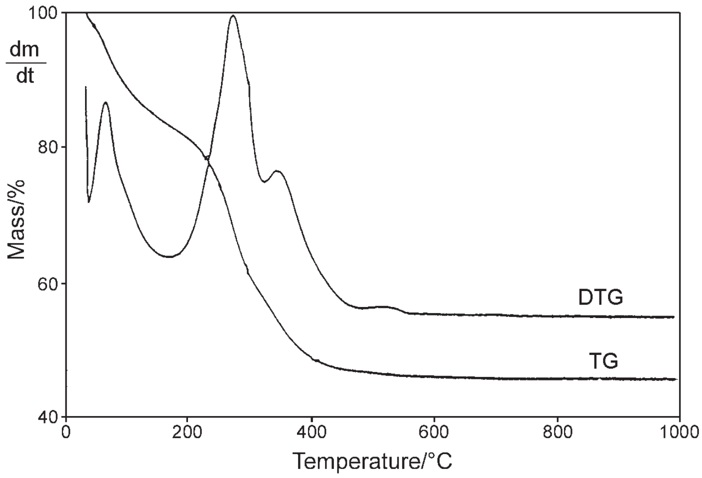

Fig. 2c TG and DTG of mixture Fe–Al (I)

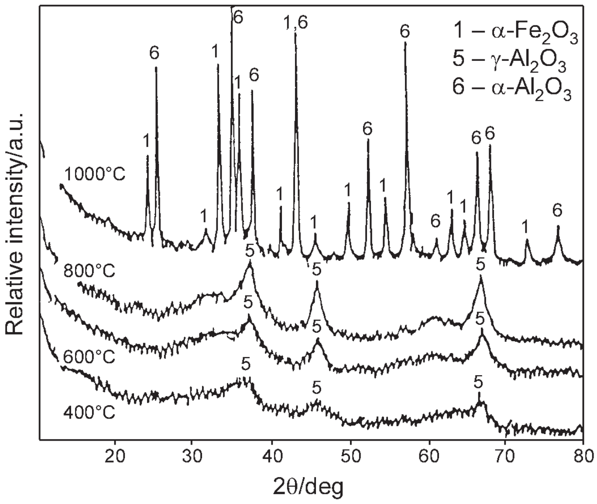

Fig. 2d XR-diffractograms of mixture Fe–Al (I) preheated at 400, 600, 800 and 1000°C

its surface and hindering their grain growth. On the other hand, further increase of calcination temperature up to 1000°C, yielded a crystalline manganese aluminate phases as a result of solid–solid interaction between the thermal products according to the following equation:

$$Mn_2O_3+2Al_2O_3 \rightarrow 2MnAl_2O_4+\tfrac{1}{2}O_2 \qquad (1)$$

Also, crystalline Mn_3O_4 and α-Al_2O_3 were detected. The formation of the later phase reflects the role of manganese oxide which enhance the ordering process of alumina in the alpha form [7, 17] at this temperature.

Thermal analysis and XRD-characterization of mixture Fe–Al (VI)

Figure 2c shows three steps for the thermal decomposition of the mixture Fe–Al (VI) which accompanied by total mass losses of 15.5, 59.0 and 60.5%. The first step corresponds to the loss of all water from the mixture and starting the decomposition of aluminum hydroxide to aluminum oxyhydroxide at about 215°C. The second step starts at 405°C reaching a constant total mass loss of 59.0% which might correspond to the complete decomposition of aluminum hydroxide to aluminum oxide and the formation of Fe(OOH) compound. The last step starts at about 530°C with a total mass loss of 60.5% corresponding to the complete decomposition of the mixture Fe–Al (VI) to Fe_2O_3 and Al_2O_3. This means that the presence of aluminum retarded the decomposition of ferric nitrate to ferric oxide. In contrast, the presence of iron enhanced the thermal decomposition of aluminum hydroxide to Al_2O_3.

The X-ray investigation of the mixture Fe–Al (VI) preheated at 400, 600, 800 and 1000°C is shown in Fig. 2d. It can be seen that no patterns of ferric oxide are detected up to 800°C. On the one hand, crystalline γ-Al_2O_3 phase was detected from 400 up to 800°C. In this case, alumina acts as support and greatly increases the degree of dispersion and hinders the grain growth of the ferric oxide constituents. On the other hand, the thermal treatment of the mixture at 1000°C, led to the formation of well crystallized α-Fe_2O_3 phase. This phase enhanced the crystallization of Al_2O_3 in alpha form at this temperature.

Thermal analysis of pure mixtures of Mn–Al (I) and Fe–Al (IV) influenced by doping with ferric and manganese oxides, respectively

The thermal analyses of the pure mixtures of Mn–Al (I) influenced by doping with ferric oxide; symbolized by Fe–Mn–Al (IV) and Fe–Mn–Al (V); are represented in Figs 3a and 3b. The thermal analysis of the mixture, Fe–Al (I) influenced by doping with manganese oxide; symbolized by Mn–Fe–Al (IX) and Mn–Fe–Al (X); is represented in Figs 3c and 3d. From these figures, it can be seen that the main difference between them is that the DTG-curves of the mixtures (IV and V) showed two main peaks their maxima temperatures being located at about 550 and 880°C. These peaks were accompanied by total mass loss of 46% corresponding to the reduction of MnO_2 to Mn_2O_3 and the formation of Al_2O_3 beside Fe_2O_3 at about 550°C. The last thermal decomposition step starts at about 870°C and followed by a mass loss of 1.0%, which might represent the formation of Mn_3O_4, $MnAl_2O_4$ and Fe_3O_4. These phases will be confirmed later by XRD investigation.

On the other hand, the DTG-curves of the mixtures Mn–Fe–Al (IX and X) did not detect the peaks located at 550 and 880°C. Also, the TG-curves of these mixtures did not show a noticeable mass loss up to 1000°C. From the above results, it could be concluded that the presence of iron enhanced the thermal decomposition of aluminum hydroxide to aluminum oxide and manganese nitrate to manganese trioxide and stabilized the latter phase up to high temperature. So, the probability of the formation of manganese ferrite is possible, which will be confirmed later by the XRD investiga-

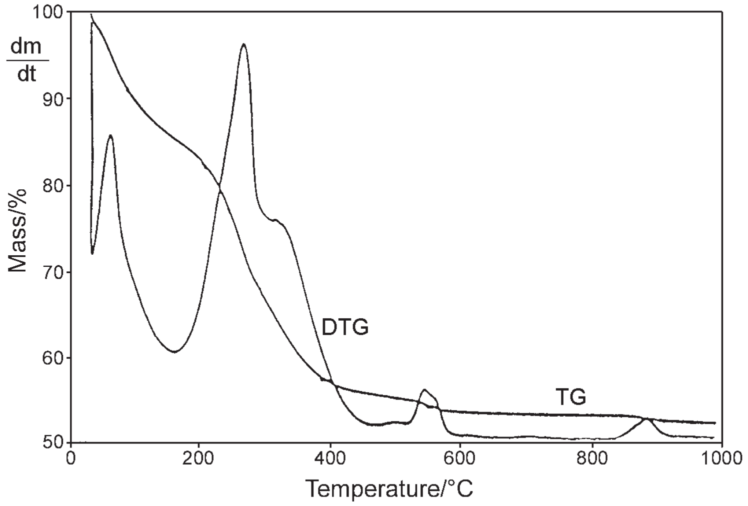

Fig. 3a TG and DTG of mixture Fe–Mn–Al (IV)

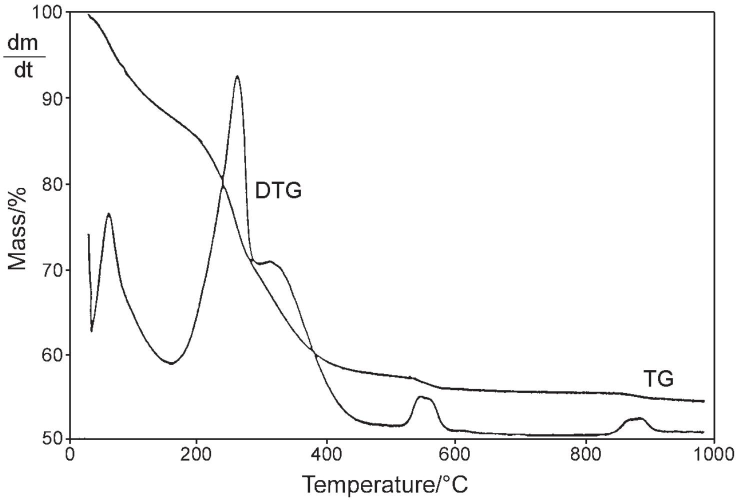

Fig. 3b TG and DTG of mixture Fe–Mn–Al (V)

tion of the mixtures (IX and X) precalcined at 1000°C. These results reflect the effect of sequence in the preparation process on the thermal decomposition course.

XRD-characterization of mixtures of Mn–Al (I) and Fe–Al (VI) influenced by doping with ferric and manganese oxides and preheated at 400–800°C

Figures 4a–d show the X-ray diffractograms of the mixtures Fe–Mn–Al (IV and V) and Mn–Fe–Al (IX and X) thermally treated at 400, 600 and 800°C. From these figures it can be seen that the treatment of all mixtures at 400°C showed the formation of

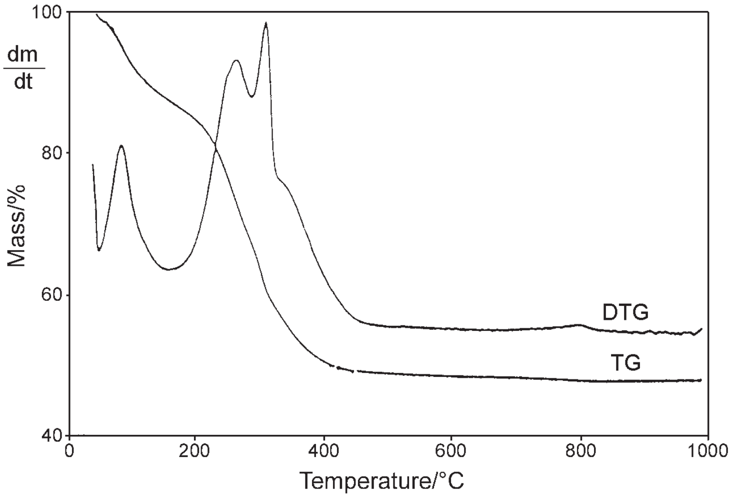

Fig. 3c TG and DTG of mixture Mn–Fe–Al (IX)

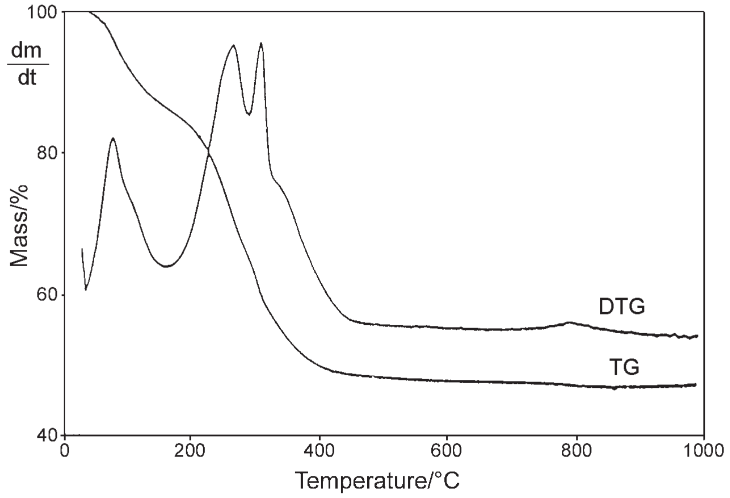

Fig. 3d TG and DTG of mixture Mn–Fe–Al (X)

poor crystalline γ-Al_2O_3 phases. It can be noticed that the degree of crystallinity of the formed phases decreased with increasing the amount of ferric oxide added to the pure mixture Mn–Al (I) and a progressive decrease was observed when manganese oxide doped the mixture Fe–Al (VI). At the same time, well crystallized β-MnO_2 phase was detected for all the mixtures preheated at 400°C except for the mixtures Mn–Fe–Al (IX and X) precalcined at the same temperature.

The thermal treatment of the above mixtures at 600 and 800°C led to the formation of only two crystalline Mn_2O_3 cubic phase beside γ-Al_2O_3 phases. There are no patterns detected for the ferric oxide as a separate phase for all the mixtures thermally treated at

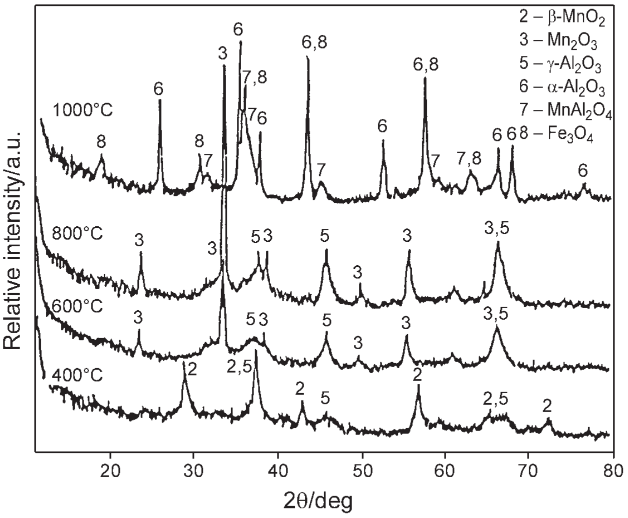

Fig. 4a XR-diffractograms of mixture Fe–Mn–Al (IV) preheated at 400, 600, 800 and 1000°C

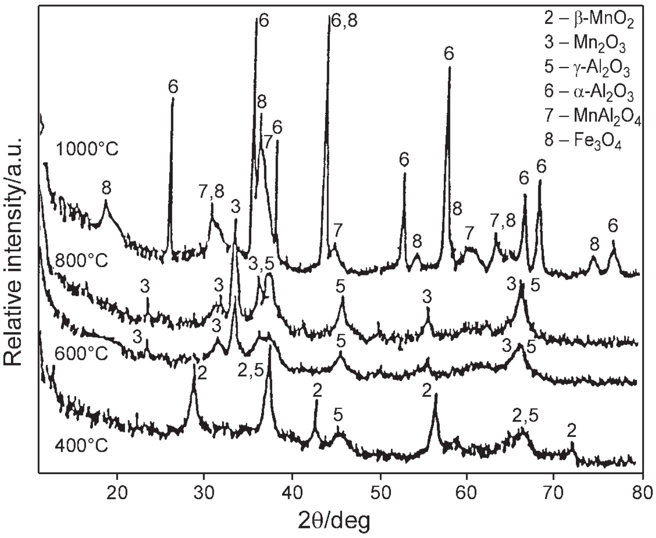

Fig. 4b XR-diffractograms of mixture Fe–Mn–Al (V) preheated at 400, 600, 800 and 1000°C

400 up to 800°C. This behavior is in contrast to that of pure ferric nitrate preheated at the same temperatures and reflects the role [17] of Al_2O_3 in increasing the degree of dispersion of Fe_2O_3 crystallites; in other words, Al_2O_3 much decreased the particle size of Fe_2O_3 phase to an extent preventing its detection in the XRD investigation. Furthermore, the intensity of Mn_2O_3 patterns was found to decrease with increasing the ferric oxide content

in the mixture. Also, it can be seen that the degree of crystallinity of the observed phases increased with increasing the calcination temperature up to 1000°C.

XRD-characterization of mixtures of Mn–Al (I) and Fe–Al (VI) influenced by doping with ferric and manganese oxides and preheated at 1000°C

From Figs 4a–d it can be seen that the mixtures Fe–Mn–Al (IV and V) doped with ferric oxide and preheated at 1000°C showed the formation of well crystalline α-Al_2O_3, $MnAl_2O_4$ and Fe_3O_4 phases. On the other hand, the X-ray of the mixtures

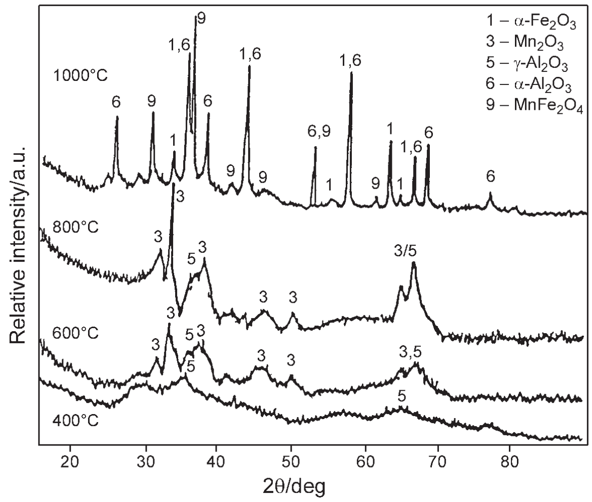

Fig. 4c XR-diffractograms of mixture Mn–Fe–Al (IX) preheated at 400, 600, 800 and 1000°C

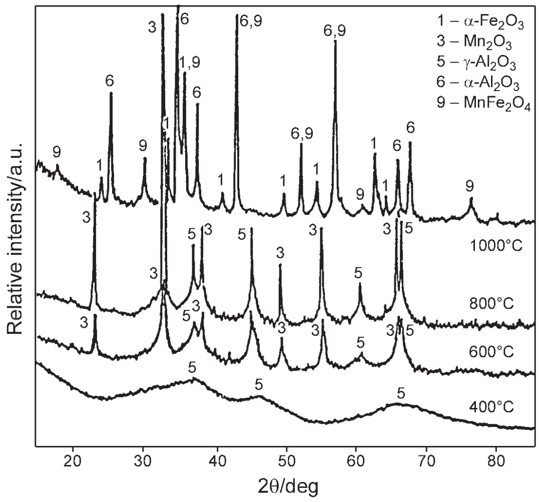

Fig. 4d XR-diffractograms of mixture Mn–Fe–Al (X) preheated at 400, 600, 800 and 1000°C

Mn–Fe–Al (IX and X) doped with manganese oxide and thermally treated at the same temperature showed the formation of well crystalline α-Al_2O_3, α-Fe_2O_3 and $MnFe_2O_4$ phases. The above results reflect the role of both of manganese and ferric oxides to enhance the crystallization process of alumina in the alpha form at temperature lower than its formation (>1200°C) [7, 17].

Comparing the obtained results of XRD of the mixture Mn–Al (I) and that doped with ferric oxide; mixtures (IV and V); preheated at 1000°C. It can be seen that the crystalline Mn_3O_4 phase was detected only for the mixture Mn–Al (I). This behaviour reflects the role of ferric oxide to stabilize the manganese trioxide, which may undergo solid–solid interaction with alumina forming manganese aluminate as previously mentioned. The degree of intensity manganese aluminate phase increase with increasing the ferric oxide content in the mixture. The absence of manganese ferrite phase in the case of mixtures (IV and V) is quite expected due to the absence of any free manganese oxide and also the formation of crystalline Fe_3O_4 phase at this temperature (1000°C). It seems that the crystallization of Fe_2O_3 into Fe_3O_4 might suggest that the formation of manganese aluminate enhanced the phase transformation process as follows:

$$3Fe_2O_3 \xrightarrow{1000\,^\circ C;\ (MnAl_2O_4)} 2Fe_3O_4+1/2O_2 \qquad (2)$$

So, it can be seen that both of manganese aluminate and Fe_3O_4 have mutual effect on the formation of each other, at the same time, their formation is quite correlated with the absence of manganese ferrite for the mixtures (IV and V) preheated at 1000°C. Moreover, the X-ray diffractogram of the mixtures (IX and X) precalcined at 1000°C showed the absence of crystalline Mn_3O_4, $MnAl_2O_4$ and Fe_3O_4 phases. In this case, iron was added before manganese to alumina, so, the formed ferric oxide coverage the surface of alumina and acted as energy barrier for manganese oxide to interact with Al_2O_3 and hence the disappearance of $MnAl_2O_4$ phase, which affects the formation of Fe_3O_4 as mentioned previously, and then a portion of the produced small-sized Fe_2O_3 crystallites undergo solid–solid interaction with the manganese oxide forming crystalline manganese ferrite phase according to the following equation [12, 18].

$$Mn_2O_3+2Fe_2O_3 \xrightarrow{1000\,^\circ C} 2MnFe_2O_4+O_2 \qquad (3)$$

Catalytic activities measurements

Table 2 shows that the rate constant (k/min^{-1}) of hydrogen peroxide decomposition reaction over single oxides obtained by calcination of their salts at 400–800°C are lower than that of mixed and doped oxides supported on alumina. In most cases, it could be seen that the catalytic activity increased with increasing the reaction temperature from 30 up to 50°C.

Table 2 The dependence of rate constant (k·10/min^{-1}) on the catalyst composition, calcination temperatures and reaction temperatures

Catalysts from	Calcination temperature/°C	k·10/min^{-1}			ln$A$	E/ kJ mol^{-1}
		30°C	40°C	50°C		
$Mn(NO)_3 \cdot 4H_2O$	400	1.5	1.7	2.2	6	20
	600	1.0	1.5	1.9	9	28
	800	0.6	1.1	1.5	13	40
Mn–Al (I)	400	2.6	3.3	4.7	8	24
	600	3.2	5.0	7.9	14	37
	800	4.0	6.2	9.9	15	40
0.025Fe–Mn–Al (II)	400	3.4	5.2	8.4	14	37
	600	4.1	7.5	10.8	15	40
	800	5.1	9.0	14.0	21	54
0.05Fe–Mn–Al (III)	400	2.1	3.0	4.3	10	29
	600	2.7	4.4	6.3	13	35
	800	4.1	5.4	8.5	11	31
0.10Fe–Mn–Al (IV)	400	1.5	2.4	3.4	11	33
	600	1.3	1.8	2.3	8	25
	800	0.8	1.2	1.7	11	34
0.25Fe–Mn–Al (V)	400	0.9	1.3	1.8	10	32
	600	0.4	0.7	1.1	13	42
	800	0.2	0.4	0.7	16	50
Fe–Al (VI)	400	0.3	0.4	0.5	8	31
	600	0.1	0.2	0.20	8	33
	800	0.06	0.1	0.14	9	35
0.025Mn–Fe–Al (VII)	400	0.8	1.3	1.8	12	36
	600	0.4	0.6	0.9	12	38
	800	0.2	0.4	0.7	16	50
0.05Mn–Fe–Al (VIII)	400	1.0	1.7	3.2	17	49
	600	0.6	1.1	1.8	15	46
	800	0.33	0.6	1.0	13	46
0.10Mn–Fe–Al (IX)	400	1.39	1.9	2.60	8	26
	600	0.86	1.4	2.05	12	36
	800	0.44	1.0	1.48	17	50
0.25Mn–Fe–Al (X)	400	2.20	3.0	4.00	9	25
	600	1.43	2.0	3.10	11	33
	800	0.60	1.0	1.12	8	26
$Fe(NO_3)_3 \cdot 9H_2O$	400	0.06	0.2	0.20	15	50
	600	0.03	0.1	0.16	22	69
	800	0.01	0.04	0.07	26	80

Catalytic activity of single oxides

The experimental results of the catalytic decomposition of H_2O_2 over hydrated ferric nitrate and aluminum hydroxide preheated at 400–1000°C did not show noticeable catalytic activity because of the formation of inactive species of Fe_2O_3 and Al_2O_3 [12, 17]. On the other hand, pure manganese nitrate preheated at 400 and 600°C showed high catalytic activity, which is attributed to the formation of MnO_2 and Mn_2O_3 respectively. On further increase of treatment temperature up to 1000°C, the activity sharply decreased, because of the increasing of degree of crystallinity of active species, formation of Mn_3O_4 and/or sintering process [10, 19].

Catalytic activity of pure Mn oxide/Al_2O_3 and Fe_2O_3/Al_2O_3 systems

Table 2 shows that the rate of hydrogen peroxide decomposition reaction over Mn oxide/Al_2O_3 system obtained at different temperatures increased with increasing the treatment up to 800°C and also increased with increasing the reaction temperatures from 30 up to 50°C. The X-ray results of this solid preheated at 400 and 600°C possess phases of MnO_2 and Mn_2O_3, which are very active in this reaction. In this case, according to Kanungo *et al.* [20], the decomposition may take place by donating an electron from the substrate to the solution or vice versa. Then, if the catalyst accepts an electron, the possible active site is Mn^{4+} to yield a $H\dot{O}_2$ radical according to the following equation:

$$Mn^{4+}+H_2O_2 \rightarrow H^{+}+H\dot{O}_2+Mn^{3+} \tag{4}$$

The observed increase in the activity of Mn_2O_3/Al_2O_3 system due to heating at 800°C might be attributed to a possible formation of metal oxide/support compound. This system possesses an activity higher than that of the pure oxides obtained at the same calcination temperatures. Because, these conditions favour the increase of the active site concentration of manganese trivalent which yield an $^{\bullet}OH$ radical as follows:

$$Mn^{3+}+H_2O \rightarrow {}^{\bullet}OH+HO^{-}+Mn^{4+} \tag{5}$$

Furthermore, it can be observed from Table 2 that the rate of H_2O_2 decomposition over Fe_2O_3/Al_2O_3 system obtained at different treatment temperatures was found to be much lower than that of Mn_2O_3/Al_2O_3. However, the activity of this system is higher than that of pure ferric nitrate preheated at the same. temperatures. This is explained in term that, alumina greatly increases the degree of dispersion of active constituents hindering their grain growth and thus increasing the activity of the supported system by increasing the concentration of catalytically active constituents of Mn^{3+}–Mn^{2+} or Fe^{3+}–Fe^{2+} ion pairs [10, 21].

Effect of Fe_2O_3 doping on the activity of Mn oxide/Al_2O_3 systems

The effect of Fe_2O_3 doping on Mn oxide/Al_2O_3 system obtained at reaction temperatures ranging between 400–800°C has been represented in Fig. 5a. This figure shows that the catalytic activity of Mn oxide/Al_2O_3 system obtained at different calcination temperatures (400–800°C) increases progressively by increasing the amount of dopant present reaching a maximum limit at 1.96 mol%, then significant decrease by increasing the dopant concentration above this limit was observed. The observed increase in the activity can express the induced increase with concentration of catalytically active constituents taking

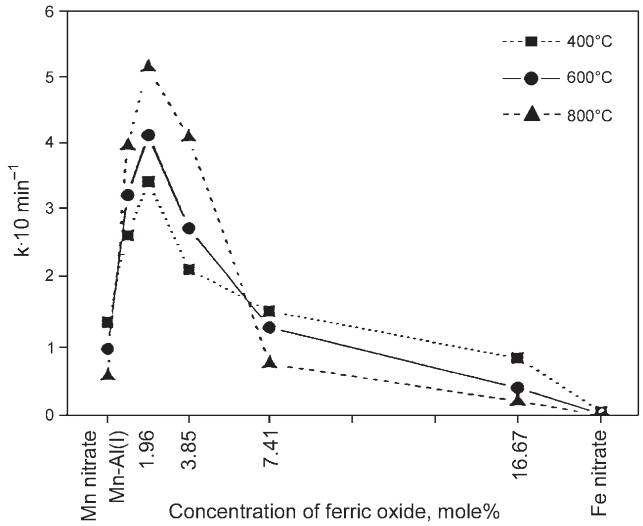

Fig. 5a Effect of Fe_2O_3 doping on the catalitic activity of Mn oxide/Al_2O_3 systems at three different temperatures

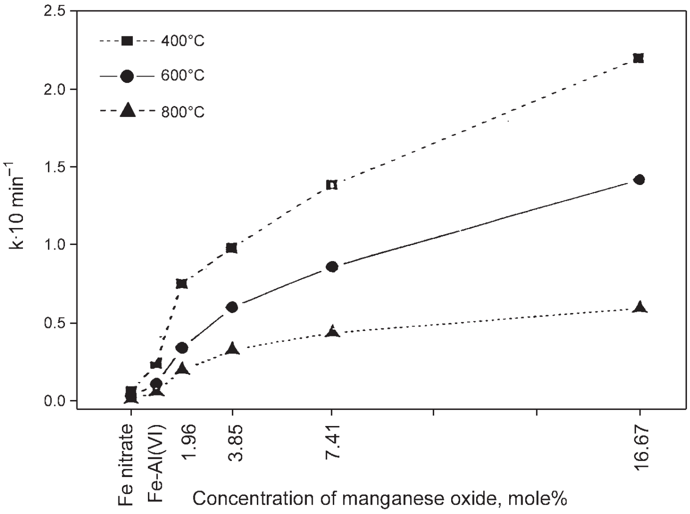

Fig. 5b Effect of Mn oxide doping on the catalitic activity of Fe_2O_3/Al_2O_3 systems at three different temperatures

part in the catalysis of H_2O_2 decomposition reaction. This assumption is evidenced from the fact that ΔE; clustered in Table 2; is dependent on the (A) term of the exponential factor in Arrhenius equation. The created active sites due to ferric oxide doping could be Fe^{3+}–Mn^{3+}, Fe^{3+}–Mn^{2+}, Fe^{3+}–Fe^{2+}, Mn^{3+}–Mn^{2+} ion pairs. However, the observed significant decrease in the catalytic activity on increasing the ferric oxide doping; from 3.85 to 16.67 mol%; which might be attributed to the decrease of the concentration of the highly active species of manganese due to the process of blocking of this active constituents by the high concentration of small active dopant.

Effect of Mn oxide doping on the activity of Fe_2O_3/Al_2O_3 system

In contrast to the above case, Fig. 5b shows that the loading of the manganese oxide on Fe_2O_3/Al_2O_3 system obtained at 400–800°C significantly increased the catalytic activity of the system on increasing the concentration of dopant from 1.96 to 16.67 mol% at different treatment temperatures. This may be attributed to the role of manganese species previously mentioned. In this case the concentration of active species; specially of manganese sites; progressively increased leading to increase the activity. From Table 2 it can be seen that ΔE values increase on increasing the amount of manganese oxide species.

Finally, it was found that the catalytic activity of all the solids thermally treated at 1000°C sharply decreased. This may be attributed to the formation of inactive species such as $MnAl_2O_4$, $MnFe_2O_4$ and/or sintering process [10, 15].

Conclusions

- Pure manganese nitrate yields MnO_2 at 300°C and Mn_2O_3 at 500°C and Mn_3O_4 at 1000°C while ferric nitrate decomposed to Fe_2O_3 at 350°C and showed thermal stability up to 1000°C.
- Ferric oxide dopant enhanced the thermal decomposition of aluminum hydroxide to aluminum oxide. Both of ferric and manganese oxides enhanced the crystallization process of aluminum oxide in the alpha form at 1000°C.
- Ferric oxide dopant enhanced the catalytic activity of Mn oxide/Al_2O_3 system obtained at 400–800°C up to certain limit of dopant then it progressively decreased on further increase of the dopant concentration.
- Crystalline manganese aluminate and manganese ferrite phases were formed as a result of thermal solid–solid interaction between the corresponding oxides at 1000°C. These phases affect the phase transformation of Fe_2O_3 to Fe_3O_4 in the mixed solids precalcined at 1000°C.
- Aluminum hydroxide retarded the thermal decomposition of ferric nitrate to ferric oxide and also retarded the decomposition of manganese nitrate to manganese dioxide.
- The catalytic activity of Fe_2O_3/Al_2O_3 system progressively increased with increasing the manganese oxide dopant concentration.

References

1 A. M. Donia, N. R. E. Radwan and A. A. Attia, J. Thermal Anal. Cal., 61 (2000) 249.
2 G. A. El-Shobaky and G. A. Fagel, Thermochim. Acta, 141 (1989) 205.
3 F. Lony and J. Valyon, J. Therm. Anal. Cal., 46 (1996) 211.

4 M. Kurzawa and G. Dabrowska, J. Therm. Anal. Cal., 60 (2000) 183.
5 H. G. El-Shobaky, M. Mokhtar and A. S. Ahmed, Thermochim. Acta, 39 (1999) 327.
6 M. I. Zaki, A. K. H. Nohman, G. A. M. Hussein and Y. E. Nashed, J. Mater. Sci. Lett., 14,17 (1995) 118.
7 M. Planda and P. Staszuk, J. Therm. Anal. Cal., 62 (2000) 561.
8 L. Lycourghiotis, V. Dimitris and A. Nicholas, Z. Phys. Chem., 125 (1998) 95.
9 G. A. El-Shobaky and A. N. Noaimi, Surf. Technol., 26 (1985) 235.
10 W. M. Shaheen and M. M. Selim, Thermochim. Acta, 322 (1998) 117.
11 K. Wieczorek-Ciuowa and A. J. Kozak, J. Therm. Anal. Cal., 58 (1999) 647.
12 M. M. Selim and L. B. Khalil, Afinidad, 48 (1991) 167.
13 W. M. Shaheen and M. M. Selim, J. Therm. Anal. Cal., 59 (2000) 961.
14 M. M. Selim and M. K. El-Aiashy, Materials Letters, 21 (1995) 262.
15 M. M. Selim, N. A. Hassan, W. Mokhtar and A. A. Attia, Bull. NRC, Egypt, 21 (1996) 1.
16 W. M. Shaheen and M. M. Selim, Afinidad, LVI, 479 (1999) 39.
17 G. A. El-Shobaky, G. A. Fagal, N. Petro and A. M. Dessouki, Radiation Physics and Chemistry, 29 (1987) 39.
18 T. Konvička, P. Mošner and Z. Šolc, J. Therm. Anal. Cal., (2000) 629.
19 V. Mucka and K. Lang, Collect. Chem. Common, 33 (1988) 1836.
20 S. B. Kanungo, K. M. Parida and B. R. Sant, Electrochim. Acta, 26 (1981) 1157.
21 V. Mucka, Collect. Chem. Common, 51 (1986) 1874.